JCI The Journal of Clinical Investigation

LKB1 loss promotes endometrial cancer progression via CCL2-dependent macrophage recruitment

Christopher G. Peña, … , Rolf A. Brekken, Diego H. Castrillon

J Clin Invest. 2015;125(11):4063-4076. https://doi.org/10.1172/JCI82152.

Research Article **Oncology**

Endometrial cancer is the most common gynecologic malignancy and the fourth most common malignancy in women. For most patients in whom the disease is confined to the uterus, treatment results in successful remission; however, there are no curative treatments for tumors that have progressed beyond the uterus. The serine/threonine kinase LKB1 has been identified as a potent suppressor of uterine cancer, but the biological modes of action of LKB1 in this context remain incompletely understood. Here, we have shown that LKB1 suppresses tumor progression by altering gene expression in the tumor microenvironment. We determined that LKB1 inactivation results in abnormal, cell-autonomous production of the inflammatory cytokine chemokine (C-C motif) ligand 2 (CCL2) within tumors, which leads to increased recruitment of macrophages with prominent tumor-promoting activities. Inactivation of *Ccl2* in an *Lkb1*-driven mouse model of endometrial cancer slowed tumor progression and increased survival. In human primary endometrial cancers, loss of LKB1 protein was strongly associated with increased CCL2 expression by tumor cells as well as increased macrophage density in the tumor microenvironment. These data demonstrate that CCL2 is a potent effector of LKB1 loss in endometrial cancer, creating potential avenues for therapeutic opportunities.

LKB1 loss promotes endometrial cancer progression via CCL2-dependent macrophage recruitment

Christopher G. Peña,[1,2] Yuji Nakada,[1,2] Hatice D. Saatcioglu,[1,2] Gina M. Aloisio,[1,2] Ileana Cuevas,[1,2] Song Zhang,[2,3] David S. Miller,[2,4] Jayanthi S. Lea,[2,4] Kwok-Kin Wong,[5] Ralph J. DeBerardinis,[2,6] Antonio L. Amelio,[7] Rolf A. Brekken,[2,8] and Diego H. Castrillon[1,2]

[1]Department of Pathology, [2]Harold C. Simmons Comprehensive Cancer Center, [3]Department of Clinical Sciences, and [4]Department of Obstetrics and Gynecology, Division of Gynecologic Oncology, University of Texas Southwestern Medical Center, Dallas, Texas, USA. [5]Department of Medical Oncology, Dana-Farber Cancer Institute, Boston, Massachusetts, USA. [6]Children's Medical Center Research Institute, University of Texas Southwestern Medical Center, Dallas, Texas, USA. [7]Lineberger Comprehensive Cancer Center, University of North Carolina at Chapel Hill, Chapel Hill, North Carolina, USA. [8]Department of Surgery and Hamon Center for Therapeutic Oncology Research, University of Texas Southwestern Medical Center, Dallas, Texas, USA.

Endometrial cancer is the most common gynecologic malignancy and the fourth most common malignancy in women. For most patients in whom the disease is confined to the uterus, treatment results in successful remission; however, there are no curative treatments for tumors that have progressed beyond the uterus. The serine/threonine kinase LKB1 has been identified as a potent suppressor of uterine cancer, but the biological modes of action of LKB1 in this context remain incompletely understood. Here, we have shown that LKB1 suppresses tumor progression by altering gene expression in the tumor microenvironment. We determined that LKB1 inactivation results in abnormal, cell-autonomous production of the inflammatory cytokine chemokine (C-C motif) ligand 2 (CCL2) within tumors, which leads to increased recruitment of macrophages with prominent tumor-promoting activities. Inactivation of *Ccl2* in an *Lkb1*-driven mouse model of endometrial cancer slowed tumor progression and increased survival. In human primary endometrial cancers, loss of LKB1 protein was strongly associated with increased CCL2 expression by tumor cells as well as increased macrophage density in the tumor microenvironment. These data demonstrate that CCL2 is a potent effector of LKB1 loss in endometrial cancer, creating potential avenues for therapeutic opportunities.

Introduction

LKB1 (*STK11*) was initially identified as the tumor suppressor gene mutated in Peutz-Jeghers syndrome (PJS), a hereditary, autosomal dominant condition characterized by a dramatically elevated (15–20×) incidence of cancer (1, 2). Interestingly, individuals with PJS (who harbor monoallelic germline *LKB1* mutations) have a propensity to develop epithelial malignancies (i.e., carcinomas) — particularly of the lung and uterus — but not sarcomas or lymphomas (3–5). Subsequent studies found that somatic *LKB1*-inactivating mutations are common in carcinomas of diverse anatomic sites (6–8). In human tumors (8, 9) and diverse conditional mouse models (3, 6, 8, 10–12), LKB1 loss is associated with rapid disease progression and spread, leading to unfavorable clinical outcomes across tumor types. LKB1 protein stability and activity are regulated by diverse posttranslational mechanisms (13, 14), and decreased LKB1 protein expression in primary tumors in various anatomic locations correlates with poor prognosis (10, 15–18), suggesting that diverse mechanisms in addition to direct mutational inactivation can lead to loss of LKB1 activity in cancer. The *LKB1* locus (19p13.3) undergoes frequent loss of heterozygosity in cancers; for example, 19p13.3 is the most frequently deleted chromosomal region in endometrial cancer (19) and is also recurrently deleted in lung cancer (20). Monoallelic *LKB1* inactivation can lead to loss-of-function phenotypes, and *LKB1* can function as a haploinsufficient tumor suppressor locus (21).

LKB1 is a highly conserved serine/threonine master upstream kinase activating the AMPK-related family of kinases (AMPK-RKs), comprising the AMPK, BRSK, MARK, NUAK, and SIK subfamilies (5, 22). LKB1 phosphorylates the AMPK-RKs at conserved consensus sequences. The principal LKB1 phosphorylation site in AMPKα is threonine 172 (Thr172), a residue that lies in the activation loop of the AMPKα catalytic domain. Thr172 and its analogous residues in the other AMPK-RKs can also be phosphorylated by other kinases, such as CaMKKβ (23). LKB1 function is closely tied to AMPK, a regulator of cellular metabolism under conditions of energy deprivation, and some of LKB1's actions as a tumor suppressor are mediated by its control of cellular metabolism and growth via AMPK and mTOR. However, LKB1 also controls diverse biological pathways relevant to cancer via other members of the AMPK-RK family. For example, LKB1 regulates epithelial cell polarity via the MARK kinases and axon branching via the NUAK kinases (24). LKB1 also controls cell migration along extracellular matrix cues (haptotaxis) — via the MARK kinases (25). Thus, LKB1 functions as a tumor suppressor through a combination of AMPK-dependent and -independent pathways. Loss of

Note regarding evaluation of this manuscript: Manuscripts authored by scientists associated with Duke University, The University of North Carolina at Chapel Hill, Duke-NUS, and the Sanford-Burnham Medical Research Institute are handled not by members of the editorial board but rather by the science editors, who consult with selected external editors and reviewers.

Conflict of interest: Kwok-Kin Wong and Diego H. Castrillon are consultants/advisory board members of MolecularMD.

Submitted: April 27, 2015; **Accepted:** August 20, 2015.

Reference information: *J Clin Invest*. 2015;125(11):4063–4076. doi:10.1172/JCI82152.

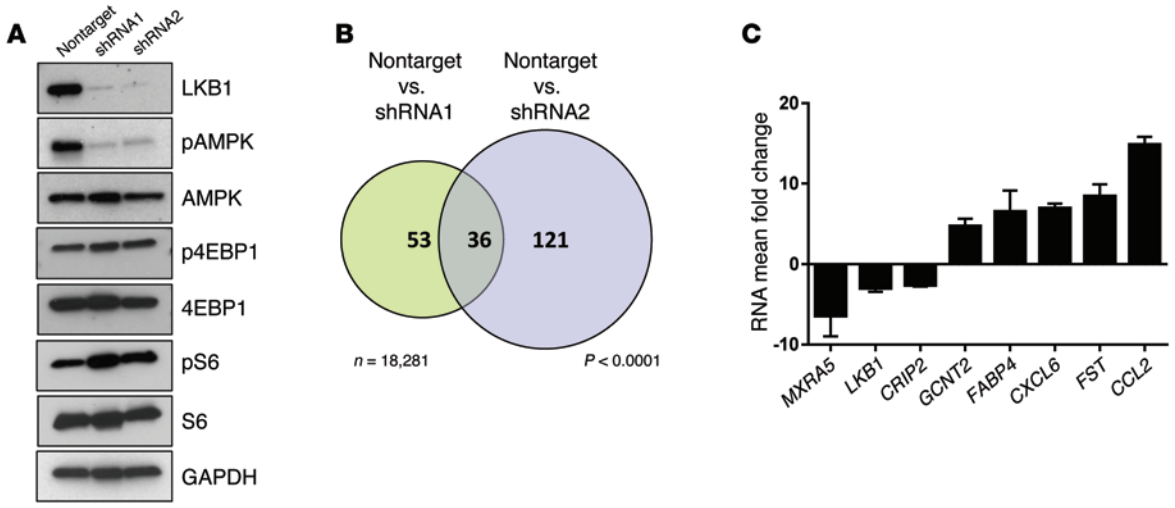

Figure 1. Discovery and validation of transcripts regulated by LKB1 in endometrial epithelium by gene-expression profiling. (**A**) Western blot of immortalized, nontransformed EM cells stably transduced with lentivirus encoding either nontarget shRNA or 1 of 2 different LKB1 shRNAs (shRNA1, shRNA2) that resulted in efficient LKB1 knockdown. LKB1 knockdown led to lower pAMPK levels, as expected, and modest effects on the levels of the phosphorylated forms of downstream mTOR-signaling components pS6 or p4EBP1. (**B**) Venn diagram of stably transduced cell lines showing the number of genes differentially expressed following LKB1 knockdown with the 2 shRNAs at a threshold of 3× or greater. $P < 0.05$ (Illumina Microarray Human HT-12 v4 BeadChip, $n = 3$ biological replicates per shRNA). There was significant overlap ($n = 35$; $P < 0.0001$ per hypergeometric test) among differentially expressed genes following shRNA1 and shRNA2 knockdown ($n = 53$ and 121, respectively, among $n = 18,281$ genes represented in microarray), demonstrating that our experimental strategy was capable of identifying bona fide LKB1 targets. (**C**) Validation of gene-expression alterations by qRT-PCR, ΔΔCt method, depicting the mean fold change of shRNA1 and shRNA2 per gene analyzed ($n = 3$ independent samples distinct from those used for microarray expression profiling). Note that all gene-expression changes were consistent with the microarray data and also that *LKB1*, which is downregulated as expected, serves as an internal control. *CCL2* showed the greatest alteration in expression levels per both microarray and RT-PCR among the subset of genes selected for validation. Error bars represent SEM.

either LKB1 or AMPK function elicits a number of cancer-associated metabolic phenotypes, including enhanced aerobic glycolysis and macromolecular biosynthesis (26).

We previously developed a mouse model of uterine cancer based on conditional inactivation of LKB1 in the endometrial epithelium. One of the remarkable properties of this model is that inactivation of a single tumor suppressor — LKB1 — is sufficient to give rise to endometrial adenocarcinomas with complete penetrance and short latency. These LKB1-deficient uterine tumors progress swiftly, leading to death in all animals (11). In contrast, most cancers require multiple cooperating mutations, and in virtually all mouse cancer models described to date, concurrent genetic "hits" are needed to give rise to invasive cancers (12). For example, homozygous inactivation of *LKB1* alone does not lead to lung cancer or even precancers, whereas *LKB1* inactivation combined with *KRAS* activation or *PTEN* inactivation provokes lung cancers with 100% incidence (6, 27). In our *LKB1*-based endometrial cancer model, pharmacologic inhibition of mTOR slowed tumor progression, implicating AMPK as an important effector of LKB1 in endometrial cancer (11). However, the aggressive nature of these LKB1-driven uterine tumors is not readily explained by misregulation of the AMPK/mTOR axis alone, particularly as the tumors were unusually well differentiated and no overt defects in cellular polarity were observed (11). These paradoxical findings and the particularly aggressive tumor progression phenotype suggested the existence of novel biological activities and unknown tumor-suppressing functions under the control of LKB1. Furthermore, several attributes of this mouse model, including its monogenic constitution, make it particularly attractive for investigations into the diverse biological manifestations of LKB1's functions as a tumor suppressor.

Unexpectedly, our human cell line studies combined with detailed analyses of this model implicated LKB1 in the control of the tumor microenvironment (TME). We found that LKB1 loss led to abnormal patterns of gene expression in endometrial epithelium characterized by misregulation of secreted factors, suggesting a novel LKB1 function in regulating the TME. Specifically, loss of LKB1 in endometrial epithelium led to the abnormal production of the proinflammatory cytokine chemokine (C-C motif) ligand 2 (CCL2). CCL2 exerted systemic effects, leading to the recruitment of protumorigenic macrophages. Finally, investigations conducted on a large number of human endometrial specimens lent further support to a model where LKB1 regulates the TME via CCL2-dependent recruitment of macrophages.

Results

Systematic identification of aberrantly expressed transcripts in endometrial epithelial cells following LKB1 loss. In addition to its previously mentioned functions, LKB1 has potent effects in shaping the cellular transcriptome through multiple mechanisms, including direct phosphorylation of cAMP response element-binding protein–regulated (CREB-regulated) transcription activators (28, 29), phosphorylation by AMPK of diverse transcriptional activators such as the forkhead box, subgroup Os (FOXOs) (30), and suppression of Snail1 (31), MYC (32), and Wnt signaling (33). We thus sought to identify transcripts whose aberrant expression follow-

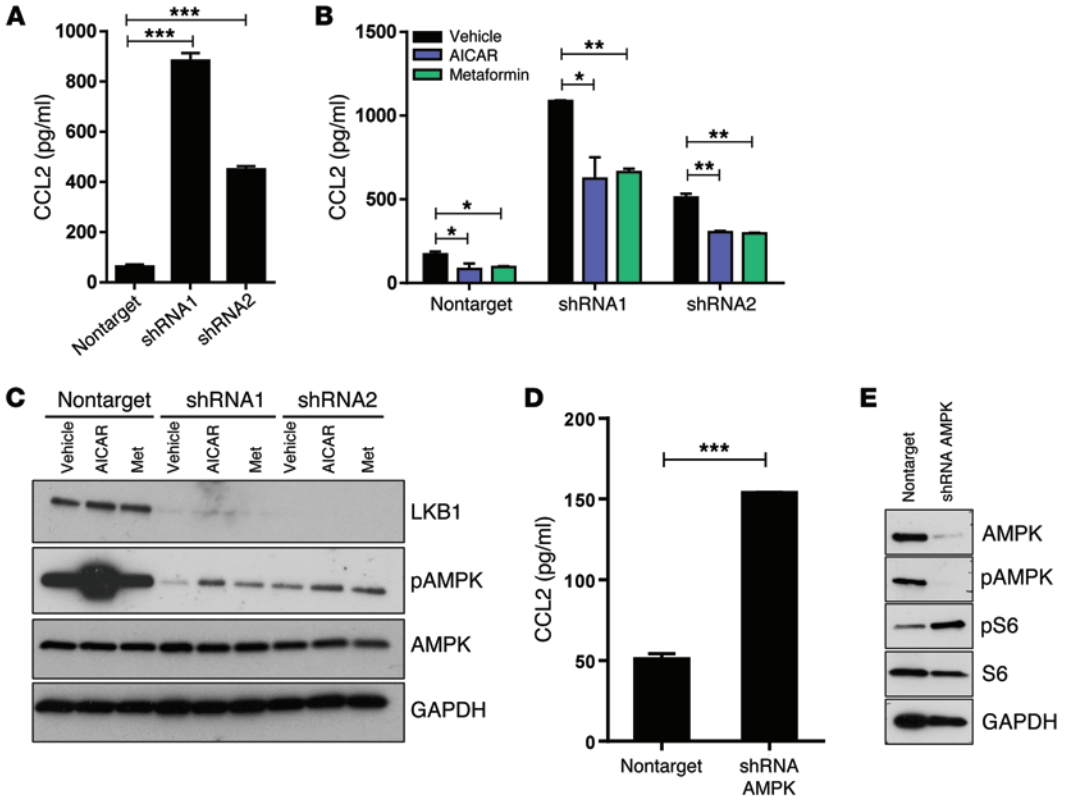

Figure 2. LKB1 suppresses CCL2 production by human EM cells via an AMPK-dependent mechanism. (**A**) Human CCL2 ELISA of conditioned media harvested 24 hours after plating of EM cells previously transduced with lentivirus. LKB1 knockdown led to a significant increase of CCL2 in the media (n = 3 biological replicates per experiment). (**B**) Human CCL2 ELISA on conditioned media containing AICAR (0.5 mM), metformin (5 mM), or vehicle (PBS) only. AICAR or metformin significantly reduced CCL2 secretion 24 hours after addition of drug (n = 3 biological replicates). (**C**) Representative Western blot of lysates from cells shown in panel **B** revealing partial restoration of pAMPK levels. (**D**) Human CCL2 ELISA on conditioned media harvested 24 hours after plating cells transduced with control or AMPKα1/2-shRNA lentivirus. AMPK knockdown led to a significant increase in CCL2 (n = 3 biological replicates per experiment). (**E**) Representative Western blot of lysates from cells shown in **D** showing knockdown of AMPK and undetectable pAMPK levels. *P < 0.05; **P < 0.001; ***P < 0.0001, Student's t test. Error bars = SEM.

ing LKB1 loss contributed to LKB1-dependent endometrial carcinogenesis. We stably transduced immortalized, nontransformed endometrial epithelial (EM) cells (34) with lentiviruses encoding either nontargeted shRNA or 1 of 2 nonoverlapping LKB1 shRNAs. Western blotting confirmed efficient LKB1 knockdown in each LKB1 shRNA cell line (shRNA1 and shRNA2) compared with the nontarget shRNA cell line (Figure 1A). As expected, LKB1 knockdown resulted in hypophosphorylation of its canonical target AMPK (at Thr172), with more modest effects on the phosphorylation status of downstream components of the AMPK/mTOR pathway (S6 and 4EBP1). Interestingly, LKB1 knockdown did not by itself result in obvious phenotypic changes in EM cells such as alterations in growth rate or motility (Supplemental Figure 1; supplemental material available online with this article; doi:10.1172/JCI82152DS1), consistent with the idea that additional genetic changes are needed to transform EM cells and in agreement with studies showing that LKB1 has a relatively modest impact on cell proliferation and instead acts as a tumor suppressor principally through its control of other biological processes (6, 35).

Total RNA was prepared from the 3 cell lines and subjected to transcriptional profiling with Illumina BeadChip Human HT-12 v4 arrays (n = 3 biological replicates per cell line, a total of 9 arrays). Signals were normalized to the nontarget controls, and transcripts exhibiting changes in abundance of more than 3× were tabulated. With these criteria, shRNA2 consistently yielded more than twice as many targets as shRNA1 (121 vs. 53), which may reflect additional "off-target" effects with shRNA2. However, more than half of the genes identified with shRNA1 (36/53, or 68%) were also identified with shRNA2, clearly demonstrating that most of the tabulated genes were deregulated as a consequence of LKB1 knockdown (Supplemental Table 1). These observations thus validated the overall gene discovery strategy of using 2 nonoverlapping shRNAs to filter out off-targets (Figure 1B, $P < 0.0001$). Notably, changes in transcript abundance for all 36 genes occurred with the same directionality (i.e., either up or down) with both shRNAs, further validating our data sets. Finally, *LKB1* itself was among the common shRNA1/2 tabulated gene sets, serving as an internal control (Supplemental Table 1).

To determine whether LKB1 regulation of the transcriptome might relate to distinct biological processes, gene ontology analysis was performed on these tabulated genes. Gene ontology terms for which significant enrichment was observed in the identified gene set included "receptor binding" ($P = 7 \times 10^{-4}$) and "structural composition of the extracellular region of cells" (i.e., secreted factors) ($P = 7 \times 10^{-6}$) (Supplemental Table 2). The regulation of some extracellular factors such as MMP12 by LKB1 in endometrial cells

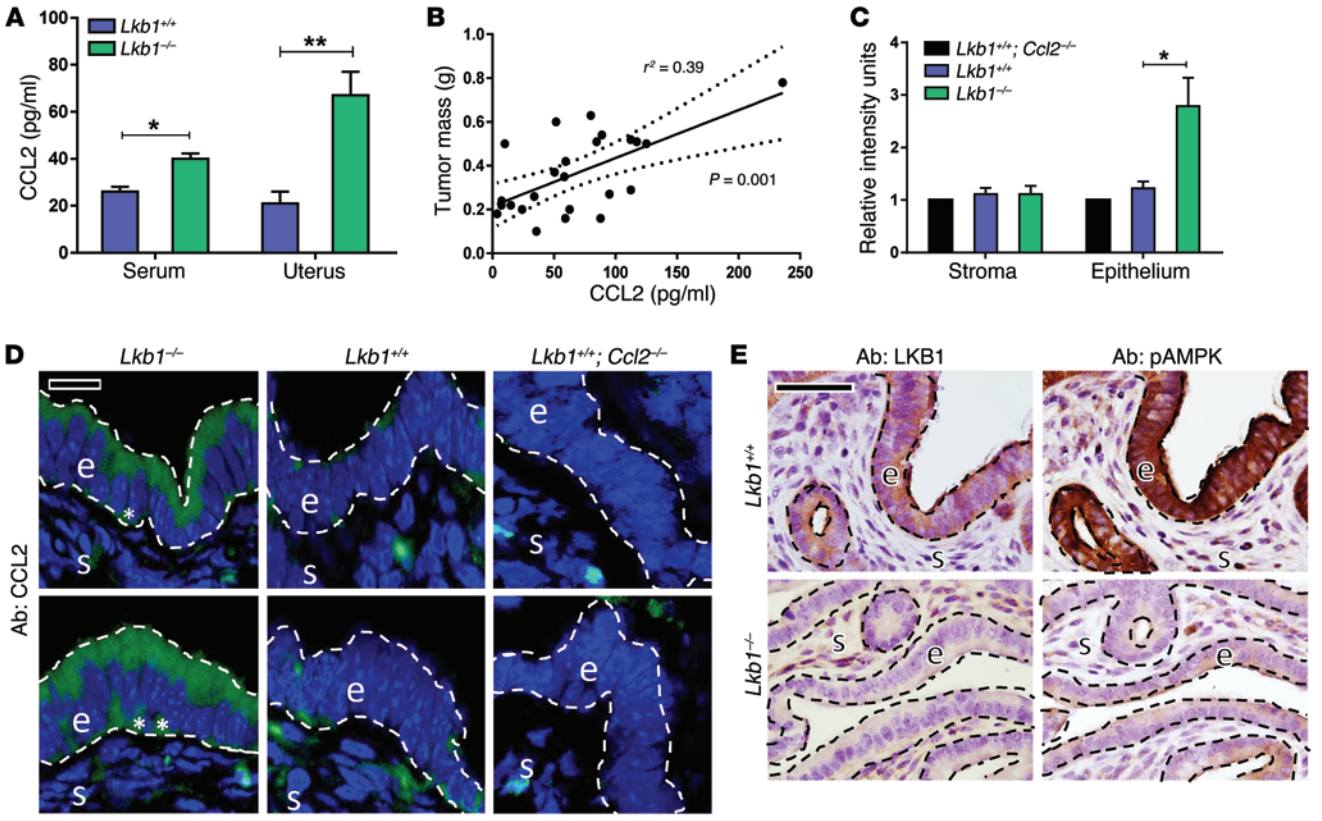

Figure 3. Conditional *Lkb1* knockout in murine endometrial epithelium results in endometrial cancers characterized by high CCL2 production. All experiments were conducted in conditional knockout *Lkb1*$^{-/-}$ and sibling control *Lkb1*$^{+/+}$ female mice at 12 weeks of age, the time point at which myometrial invasion first occurs in this well-characterized model. Tissues were harvested at proestrus. (**A**) ELISA of serum or uterine protein lysates showing a significant increase of CCL2 levels following *Lkb1* deletion (n = 14 *Lkb1*$^{+/+}$, n = 24 *Lkb1*$^{-/-}$). (**B**) CCL2 levels in tumor lysates (per ELISA) plotted against tumor mass from *Lkb1*$^{-/-}$ animals, showing a direct correlation between tumor mass and CCL2 levels (n = 24 mice, Pearson coefficient r^2 = 0.39 with P = 0.001 per 2-tailed t test). (**C**) CCL2 expression in endometrial epithelium by image analysis (regions analyzed correspond to those enclosed by dashed lines in the next panel). Tissue sections were stained with a validated CCL2 antibody, and green CCL2 signal quantitation was performed using ImageJ (http://imagej.nih.gov/ij/) (n = 6 animals per experiment). Expression was normalized to the background signal present in *Ccl2*$^{-/-}$; *Lkb1*$^{+/+}$ uterine epithelium. (**D**) CCL2 immunofluorescence of uterine tissue sections. s, stroma; e, epithelium. Asterisks denote basal CCL2 expression. Two different regions are shown for each genotype. (**E**) LKB1 and pAMPK (Thr172) immunohistochemistry of uterine tissue sections from *Lkb1*$^{+/+}$ and *Lkb1*$^{-/-}$ mice. As expected, *Lkb1* deletion in endometrial epithelium resulted in undetectable LKB1 protein as well as reduced pAMPK compared with control siblings. Statistical significance in **A** and **C** was determined by Student's t test. *P < 0.005; **P < 0.001. Scale bars: 50 μm. Error bars = SEM.

was not completely unanticipated, as prior studies have implicated LKB1 in the transcriptional regulation of secreted proteins, including tissue metalloproteases (36). Nonetheless, a significant role of LKB1 in regulating secreted chemokines such as CCL2 has not been previously documented. We also note that several genes in the common set encode factors that modulate Wnt or Hedgehog signaling (e.g., WNT2, SMOOTHENED, SFRP1), consistent with prior studies implicating LKB1 in the regulation of these pathways (33, 37); however, related gene ontology terms did not achieve statistical significance. Our results suggest a broader biological function for LKB1 in regulating the extracellular environment by secreted factors than previously anticipated.

Validation of targets deregulated following LKB1 loss and identification of the chemokine CCL2 as a biologically relevant candidate. To confirm alteration of transcript levels, we employed quantitative reverse-transcriptase PCR (qRT-PCR). Eight genes were selected for this analysis, including *LKB1* and *CCL2*, which showed the greatest fold alteration in expression levels among all genes in the Illumina analysis, as well as 6 other genes selected at random. These analyses were conducted on cells and RNA samples prepared independently from those used for the initial profiling. All 8 genes showed changes in magnitude (i.e., up or down) consistent with those observed in the Illumina BeadChip analyses (Figure 1C). These analyses also confirmed the downregulation of *LKB1* transcripts and the upregulation of *CCL2* transcripts following *LKB1* knockdown (Figure 1C).

CCL2 was a particularly intriguing candidate as a mediator of LKB1-driven endometrial tumor progression. First, the changes in CCL2 transcript levels were dramatic, more than a 10-fold increase (Supplemental Table 1 and Figure 1C). Second, CCL2 (also known as monocyte chemoattractant protein-1 [MCP-1]) is a major inflammatory chemokine with important if incompletely understood roles in tumor progression, particularly in breast and prostate cancer, where it is largely protumorigenic (38, 39). Among other functions, CCL2 is a major macrophage chemoattractant and recruits macrophages in diverse forms of tissue damage (40).

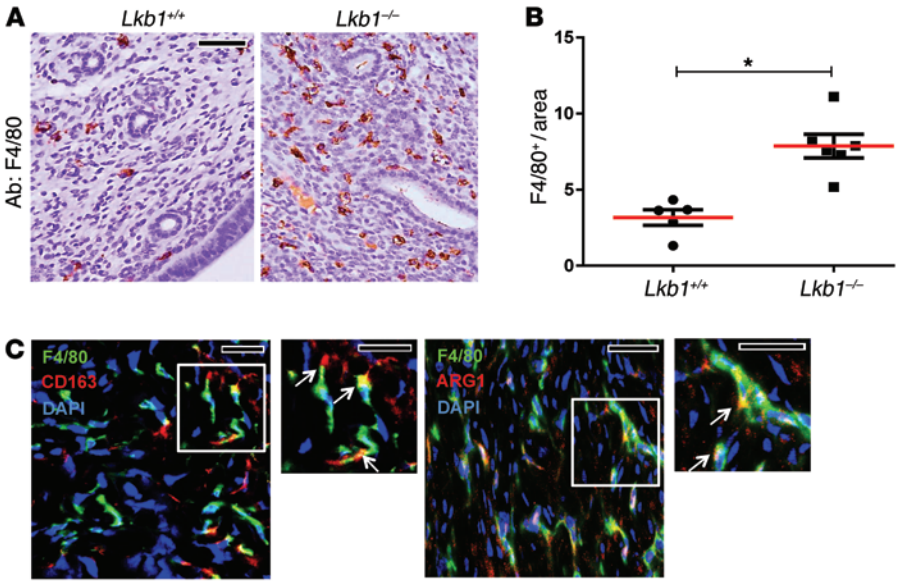

Figure 4. LKB1 loss in endometrium promotes recruitment of macrophages that express markers associated with alternative macrophage activation. Experiments were conducted in 12-week-old animals at proestrus. (**A**) Macrophage density by F4/80 immunohistochemistry. (**B**) Quantitation of macrophages in uterine tissue sections immunostained for F4/80. Positive cells were counted in 5 separate fields and normalized by total area for every mouse analyzed (n = 5 for *Lkb1*$^{+/+}$, n = 6 for *Lkb1*$^{-/-}$ mice). There were significantly increased macrophage numbers in *Lkb1*$^{-/-}$ endometrium. *P < 0.005, per Student's t test. (**C**) Presence of alternatively activated macrophages characterized by ARG1 and CD163 expression. Uterine tumor sections were stained with F4/80 and CD163 or ARG1. Arrows in the inset highlight F4/80 cells that are also positive for the other markers. Scale bars: 50 μm. Error bars = SEM.

This finding suggests that LKB1 may have an unexpected role in modulating the TME through the control of intratumoral CCL2 levels. Furthermore, the significant upregulation of a potentially protumorigenic secreted factor such as CCL2 appeared plausible as a mechanism underlying the incompletely understood tumor-promoting actions of LKB1 inactivation.

As a first step in further exploring this possibility, CCL2 ELISAs were performed on tissue culture media conditioned for 24 hours. LKB1 knockdown with shRNA1 and -2 resulted in 14× and 7.0× increased concentrations of CCL2 in the media relative to the control nontarget shRNA (Figure 2A). Furthermore, addition to the media of 5-aminoimidazole-4-carboxamide ribonucleotide (AICAR) or metformin, 2 drugs that promote the activation of AMPK (41, 42), significantly suppressed the effect of LKB1 knockdown on CCL2 levels, suggesting that LKB1 regulates CCL2 via AMPK (Figure 2B). Concordantly, AICAR and metformin also suppressed CCL2 production in the nontarget controls, further emphasizing that AMPK normally suppresses CCL2 production even when functional LKB1 is present. The restoration of pAMPK (Thr172) levels was only partial in shRNA1 and -2 knockdown cells, consistent with the fact that LKB1 is the major (but not sole) Thr172 kinase in most cells (43) and also with the observation that AICAR and metformin only partially restored CCL2 levels (Figure 2, B and C). Finally, functional inactivation of AMPK via shRNA-mediated knockdown of the catalytic subunits AMPKα(1/2) led to significantly increased CCL2 secretion (Figure 2, D and E). Thus, taken together, these results demonstrate that the LKB1/AMPK axis regulates CCL2 production within EM cells.

Misregulation of CCL2 in an Lkb1-based genetically engineered murine endometrial cancer model. To further investigate these findings in vivo, we took advantage of a well-described mouse model of endometrial cancer based on *Lkb1* ablation. In this model, homozygous deletion of *Lkb1* in endometrial epithelium with the *Sprr2f-Cre* driver results in well-differentiated but highly aggressive cancers with early invasion beginning at 12 weeks of age and all females eventually succumbing to the relentlessly progressing cancers (10, 11, 44). As previously described (11), *Sprr2f-Cre*; *Lkb1*$^{f/f}$ females (abbreviated hereafter as *Lkb1*$^{-/-}$) developed invasive endometrial adenocarcinomas beginning at 12 weeks of age, whereas sibling control *Lkb1*$^{f/f}$ females not harboring *Sprr2f-Cre* (abbreviated hereafter as *Lkb1*$^{+/+}$) never developed cancers. To study early tumor progression, mice were euthanized at 12 weeks of age, the time point coinciding with the earliest appearance of invasive cancer, but prior to the formation of advanced, bulky tumors. Per ELISA, *Lkb1*$^{-/-}$ uterine lysates contained significantly more CCL2 than *Lkb1*$^{+/+}$ sibling controls (Figure 3A). Interestingly, CCL2 levels were also increased in the peripheral blood (serum) of *Lkb1*$^{-/-}$ females, consistent with the idea that CCL2 produced by the tumorous uteri enters the circulation and thus could (a) exert systemic effects and (b) serve as a useful cancer biomarker of disease progression (Figure 3A). CCL2 concentrations showed a significant correlation with uterine tumor mass at 12 weeks of age (P = 0.001, r^2 = 0.39) (Figure 3B).

To further define the cellular source of CCL2 within uteri, tissue sections were immunostained with a validated CCL2 antibody (45). In control animals, CCL2 signals were weak, being limited to sporadic (and likely nonspecific) signals in the endometrial stromal cells and occasional faint signals in the apical cytoplasm (Figure 3D). In contrast, there was increased CCL2 immunoreactivity in *Lkb1*$^{-/-}$ uterine epithelium, predominantly in the apical cytoplasm, consistent with a secreted protein, although occasional cells exhibited some basal CCL2 localization (Figure 3D). In *Ccl2*-deficient animals (described below), the CCL2-associated signals were abolished, confirming the specificity of immunodetection in the epithelium. Image analyses (n = 6 animals per genotype) confirmed these observations (Figure 3C). Finally, we documented AMPK hypophosphorylation in the LKB1-deficient epithelium (Figure 3E), confirming that AMPK is a bona fide physiologic target of LKB1 in vivo, as previously reported (46, 47), and indicating that the observed changes in CCL2 are likely AMPK dependent, as was the case in vitro (Figure 2, B and C).

Increased macrophage recruitment in Lkb1-driven endometrial cancers and their protumorigenic role. This increased production of CCL2 and its known function as a proinflammatory chemokine

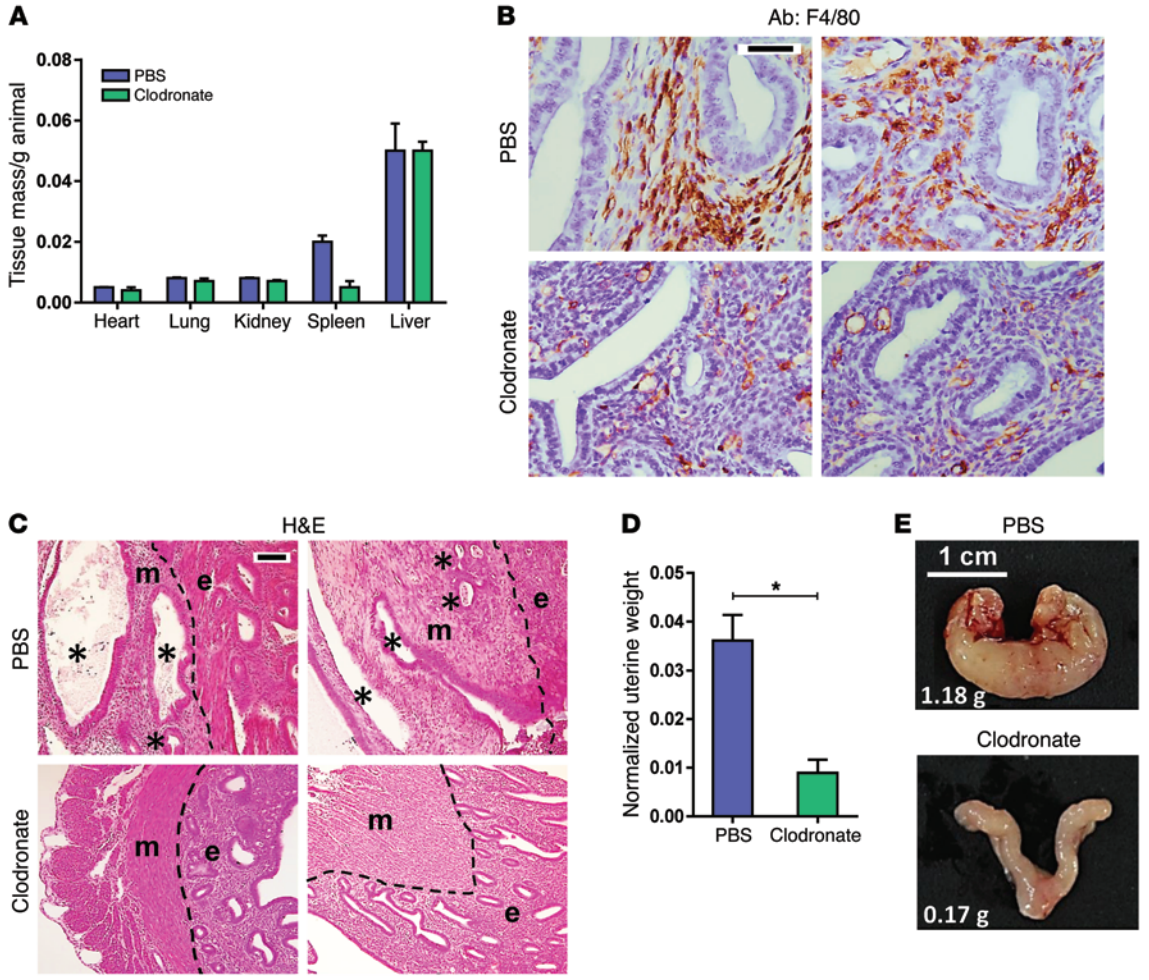

Figure 5. TAMs in *Lkb1*-driven endometrial cancers promote invasion and accelerate tumor progression. Tumor-bearing *Lkb1*$^{-/-}$ animals were treated with liposomal PBS (n = 4) or liposomal clodronate (n = 4) for 9 weeks. (**A**) Confirmation of systemic macrophage depletion. Among diverse organs, only spleen showed decrease in mass following the clodronate regimen, as expected (macrophages make up a significant percentage of cells in the spleen). (**B**) F4/80 immunohistochemistry of uterine tissue section confirming macrophage depletion following treatment with clodronate. (**C**) H&E staining showing greatly decreased myometrial invasion in clodronate-treated *Lkb1*$^{-/-}$ mice. e, endometrium; m, myometrium; dashed lines, endometrial/myometrial interface; asterisks, invasive tumor glands. Note that endometrial glands are normally present only in the endometrium; hence, the greatly decreased myometrial involvement following clodronate is consistent with slowed tumor progression. (**D**) Tumor burden, as determined by uterine weight at conclusion of treatment. There was a significant reduction in tumor mass in clodronate-treated animals. *P < 0.01, Student's t test. (**E**) Gross photographs of uteri at conclusion of treatment. Weights for uteri in grams shown in lower left-hand corner. Scale bars: 50 μm (**B** and **C**). Error bars = SEM.

led us to investigate the potential contribution of tumor-associated macrophages (TAMs) in the growth and progression of *Lkb1*-driven endometrial cancers. We employed the murine macrophage marker F4/80 to quantitate macrophage density in uterine tissue sections at 12 weeks of age. There was a significant increase (per unit area) in the number of endometrial F4/80$^+$ macrophages in *Lkb1*$^{-/-}$ mice relative to controls (Figure 4, A and B). Since the density of inflammatory cells varies throughout the murine estrus cycle (48), these studies were performed on mice at proestrus (as determined by routine exfoliated vaginal cell cytology). In contrast, tumors from 3 distinct genetically engineered mouse models of endometrial cancer characterized by loss of (a) *Pten*, (b) *Pten* and *Mig-6* (49–54), or (c) *Pot1a* and *p53* (55, 56) did not exhibit significantly increased F4/80$^+$ cells (Supplemental Figure 2, A and B), supporting the notion that elevated macrophage recruitment is a relatively specific feature of LKB1-driven endometrial cancers.

TAMs can have anti- or protumor effects depending on the tumor type, age and size of tumor, and other variables (57). It is believed that alternatively activated macrophages, known as M2 macrophages, promote tumor growth and invasion through immune suppression and local metabolic effects (58, 59). M2 macrophages can be distinguished by various markers including CD163 and arginase I (ARG1) (60). Most macrophages in *Lkb1*$^{-/-}$ tumors expressed CD163 and ARG1, suggesting that TAMs in *Lkb1* endometrial tumors are generally tumor promoting and express markers previously associated with tumor-promoting macrophage subtypes (Figure 4C).

To assess the contribution of macrophages to tumor progression, we treated *Lkb1*$^{-/-}$ mice with liposome-encapsulated clodronate, which is selectively phagocytized by macrophages, resulting in their apoptosis and depletion (61). Free clodronate (i.e., released from the dying macrophages) has an extremely short

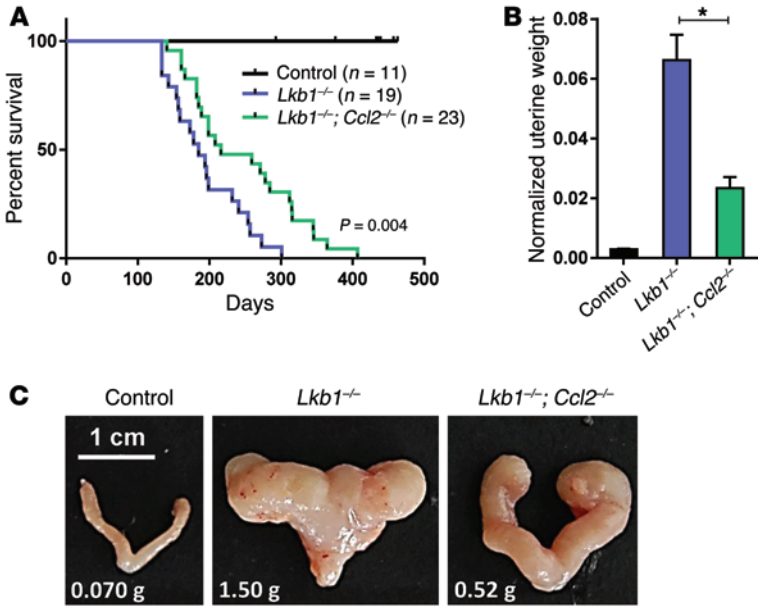

Figure 6. Endometrial cancers driven by LKB1 loss are CCL2 dependent in vivo. (**A**) Survival curves for 2 experimental genotypes and control *Lkb1*$^{+/+}$; statistical significance was calculated by log-rank test. (**B**) Tumor burden at 180 days (n = 11 *Lkb1*$^{-/-}$, n = 8 *Lkb1*$^{-/-}$; *Ccl2*$^{-/-}$) as determined by uterine weight, *P < 0.001, Student's t test (**C**) Gross photographs of uteri at 180 days of age. Weights for uteri in grams shown in lower left-hand corner. Left uterus image was cropped, rotated 180° to align uterine horns with those of the right uterus image, and the image placed on a black background. Error bars = SEM.

half-life and does not have long-term systemic effects (62). Nine-week-old females were treated with intraperitoneal injections of liposomal clodronate or liposomal PBS (control) for 9 weeks and then necropsied. The treatment was well tolerated by all animals, with no apparent side effects, deaths, or overall weight loss at any point in the treatment regimen. Among diverse control organs, only the spleen showed a reduction in weight, consistent with systemic macrophage depletion, as red pulp macrophages constitute a large cell population in spleen (Figure 5A). F4/80 immunostaining showed significantly fewer macrophages within the endometrium, confirming the effectiveness of clodronate in depleting uterine macrophages (Figure 5B).

Remarkably, macrophage depletion significantly inhibited tumor progression. Whereas invasive tumor glands were abundant and diffuse in the myometria of untreated animals at the end of the regimen (i.e. at 18 weeks of age), such invasive glands were greatly diminished following clodronate treatment (Figure 5C). Concordantly, uterine tumor burden was dramatically decreased following clodronate treatment (Figure 5D), with a 10× reduction in overall uterine tumor weights (P = 0.001), a difference readily apparent by gross examination of the tumorous uteri (Figure 5E). While *Lkb1*$^{-/-}$ tumors exhibited a modest elevation of neutrophils (but not CD3^{+} mature lymphocytes), clodronate treatment did not deplete neutrophils or lymphocytes in *Lkb1*$^{-/-}$ tumors (Supplemental Figure 3, A and B), consistent with specific depletion of macrophages and arguing that slowed tumor progression in clodronate-treated animals was due to depletion of macrophages. These experiments thus demonstrate that the TAMs recruited to *Lkb1*-driven endometrial cancers have a predominantly tumor-promoting effect.

Dependence of Lkb1-driven endometrial tumor progression on CCL2. These experiments were provocative in showing that the TAMs recruited in the context of LKB1 loss and ensuing CCL2 overproduction promote tumor progression. However, these studies did not formally establish a role of CCL2 in this process. To rigorously explore this question, an additional cohort of mice was generated by breeding *Sprr2f-Cre* and the *Lkb1* floxed allele into a *Ccl2*-deficient background. *Ccl2*-null mice, described in prior studies, are externally normal and fertile (63). Absence of circulating CCL2 in *Ccl2*$^{-/-}$ mice was confirmed by ELISA (Supplemental Figure 4A). *Sprr2f-Cre; Lkb1*$^{f/f}$*; Ccl2*$^{-/-}$ mice (hereafter abbreviated as *Lkb1*$^{-/-}$; *Ccl2*$^{-/-}$) were born at expected Mendelian ratios. A cohort of *Lkb1*$^{-/-}$; *Ccl2*$^{-/-}$ females, together with sibling *Lkb1*$^{-/-}$ and *Lkb1*$^{+/+}$ cohorts, was allowed to age for survival analysis. No tumors were observed in *Lkb1*$^{+/+}$ controls. However, loss of CCL2 increased maximal life span of *Lkb1* conditional knockout mice from 301 to 406 days, with a statistically significant extension of overall survival (P = 0.004, log-rank test) (Figure 6A). To further study tumor progression, a set of animals separate from the survival cohorts was euthanized at 26 weeks of age. Uterine tumor burden was significantly decreased (>2×) in *Lkb1*$^{-/-}$; *Ccl2*$^{-/-}$ versus *Lkb1*$^{-/-}$ females (P < 0.001; n = 11 *Lkb1*$^{-/-}$ and n = 8 *Lkb1*$^{-/-}$*; Ccl2*$^{-/-}$) (Figure 6, B and C). Thus, although genetic ablation of CCL2 did not entirely suppress the formation and progression of *Lkb1*-driven endometrial cancers, it did significantly slow the progression of these tumors, confirming that CCL2 is a critical mediator of LKB1 loss in the context of endometrial cancer growth and progression in vivo.

Uterine macrophages were further analyzed and quantitated by flow cytometry for F4/80 and CCR2, another general macrophage marker and the receptor for CCL2 (64). These analyses demonstrated that, at 26 weeks, both F4/80^{+} and F4/80^{+}/CCR2^{+} double-positive uterine macrophages were significantly decreased in *Lkb1*$^{-/-}$; *Ccl2*$^{-/-}$ versus *Lkb1*$^{-/-}$ females (Figure 7A), which was further confirmed in F4/80-immunostained uterine sections (Figure 7B). These analyses confirmed the existence of a uterine macrophage population capable of responding to CCL2 and, together with our prior observations, are consistent with the idea that CCR2^{+} macrophages play a role in tumor progression in the *Lkb1* model. Interestingly, while *Lkb1*-null mice harbored increased circulating monocytes and decreased lymphocytes, these effects were reversed by loss of CCL2 (n = 6 *Lkb1*$^{-/-}$, n = 3 *Lkb1*$^{-/-}$*; Ccl2*$^{-/-}$) (Figure 7C). Overall, these results suggest that CCL2 plays an important part in *Lkb1*-driven tumorigenesis by

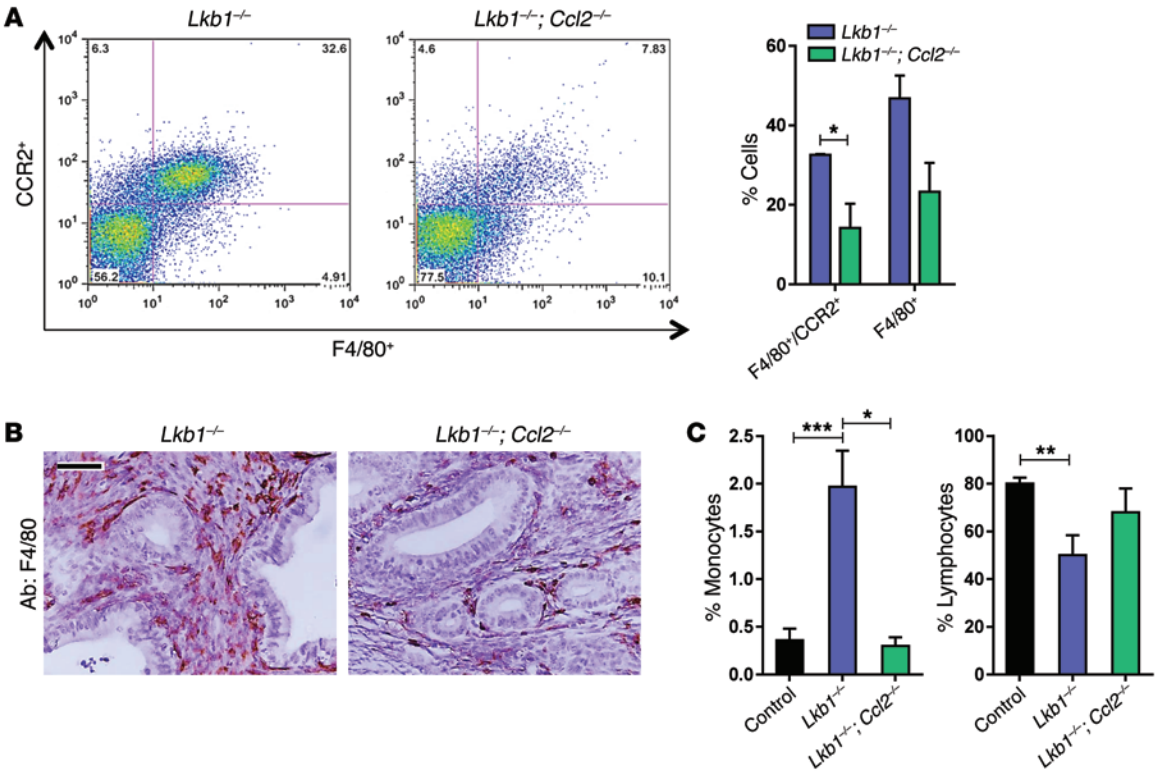

Figure 7. LKB1 tumor-associated phenotypes including recruitment of macrophages and systemic effects are CCL2 dependent. (**A**) Left: representative dot plot displaying 1 of 3 independent experiments used to quantitate F4/80$^+$/CCR2$^+$ macrophages in tumors driven by *Sprr2f-Cre* at 180 days. Right: *Lkb1*$^{-/-}$ tumorous uteri, which overexpress CCL2, contained a significantly greater percentage of F4/80$^+$/CCR2$^+$ and total F4/80$^+$ cells than *Lkb1*$^{-/-}$*; Ccl2*$^{-/-}$ tumors on average from 3 independent experiments. These data demonstrate that LKB1 loss leads to increased macrophage recruitment to the TME in a CCL2-dependent manner. (**B**) Macrophage density by F4/80 staining confirmed the presence of fewer macrophages in *Lkb1*$^{-/-}$*; Ccl2*$^{-/-}$ endometrial tumors. (**C**) Complete blood counts showing CCL2-dependent effects in circulating monocyte and lymphocyte numbers. **P* < 0.05; ***P* < 0.001; ****P* < 0.0005, Student's *t* test. Scale bars: 50 μm. Error bars = SEM.

stimulating (a) increased peripheral monocyte numbers and (b) monocyte recruitment to the endometrial tumors.

Evidence that the LKB1/CCL2/TAM axis contributes to the progression of human endometrial cancer. To study the LKB1/CCL2/TAM axis in human tumors, an endometrial cancer tissue microarray (TMA) was constructed with duplicate cores for nearly 200 independent primary tumors, predominantly of the endometrioid subtype, which is the most common (Supplemental Table 3). TMA slides were stained for CCL2, CD68 (human macrophage marker), and LKB1. Since many antibodies do not reliably detect their cognate antigen in paraffin-embedded formalin-fixed tissues (PEFFT) and few immunohistochemical (IHC) studies have been conducted on CCL2 in human PEFFT, we first validated our CCL2 IHC protocol on the Ishikawa endometrial cancer cell line overexpressing CCL2. After fixation in 10% buffered formalin followed by paraffin embedding (to simulate processing of human tissues in the clinical pathology laboratory), the CCL2-overexpressing cells gave a much higher signal than control Ishikawa cells (Supplemental Figure 5). Immunohistochemistry of serial step sections (in a subset of 10 tumors) with the macrophage-specific scavenging receptor CD163 gave virtually superimposable patterns of expression and staining scores as CD68, further validating the use of CD68 as a macrophage marker in endometrial tumors (our unpublished observations). For detection of LKB1, we employed an IHC assay previously validated for detection of endogenous LKB1 protein in PEFFT (65). Sufficient tumor was present to permit scoring of all 3 markers for $n = 175$ cases of endometrial cancer. Based on the observed patterns and intensity of staining, a semiquantitative 0–3 scoring scale was established for all 3 markers (illustrated in Supplemental Figure 6; see also Methods for detailed description of scoring criteria). Note that, while CCL2 and LKB1 IHC were used to assess protein levels in a semiquantitative manner, CD68 immunostains were used to assess macrophage density. In some primary tumors, CCL2 was expressed primarily on the apical epithelial cytoplasm, while in other tumors, CCL2 was located diffusely throughout the apical and basal cytoplasm (Supplemental Figure 6B).

After scoring was completed, heat maps were generated to explore associations among the markers. There was a strong negative association between CCL2 and LKB1, both for grade 1 and grade 1–3 endometrial cancers ($P = 0.00019$; $\tau_\kappa = -0.45$ and $P = 0.000278$; $\tau_\kappa = -0.19$ respectively). There was also a strong negative association between CD68 (i.e., macrophage density) and LKB1 scores, again in both grade 1 and grade 1–3 cancers ($P = 0.000373$; $\tau_\kappa = -0.43$ and $P = 2.72 \times 10^{-8}$; $\tau_\kappa = -0.36$, respectively) (Figure 8A).

We then categorized expression of each protein by clinical stage in addition to grade. FIGO (International Federation of Gynecology and Obstetrics, 1988) stage 1A tumors are defined by the absence of myometrial invasion, whereas 1B tumors invade

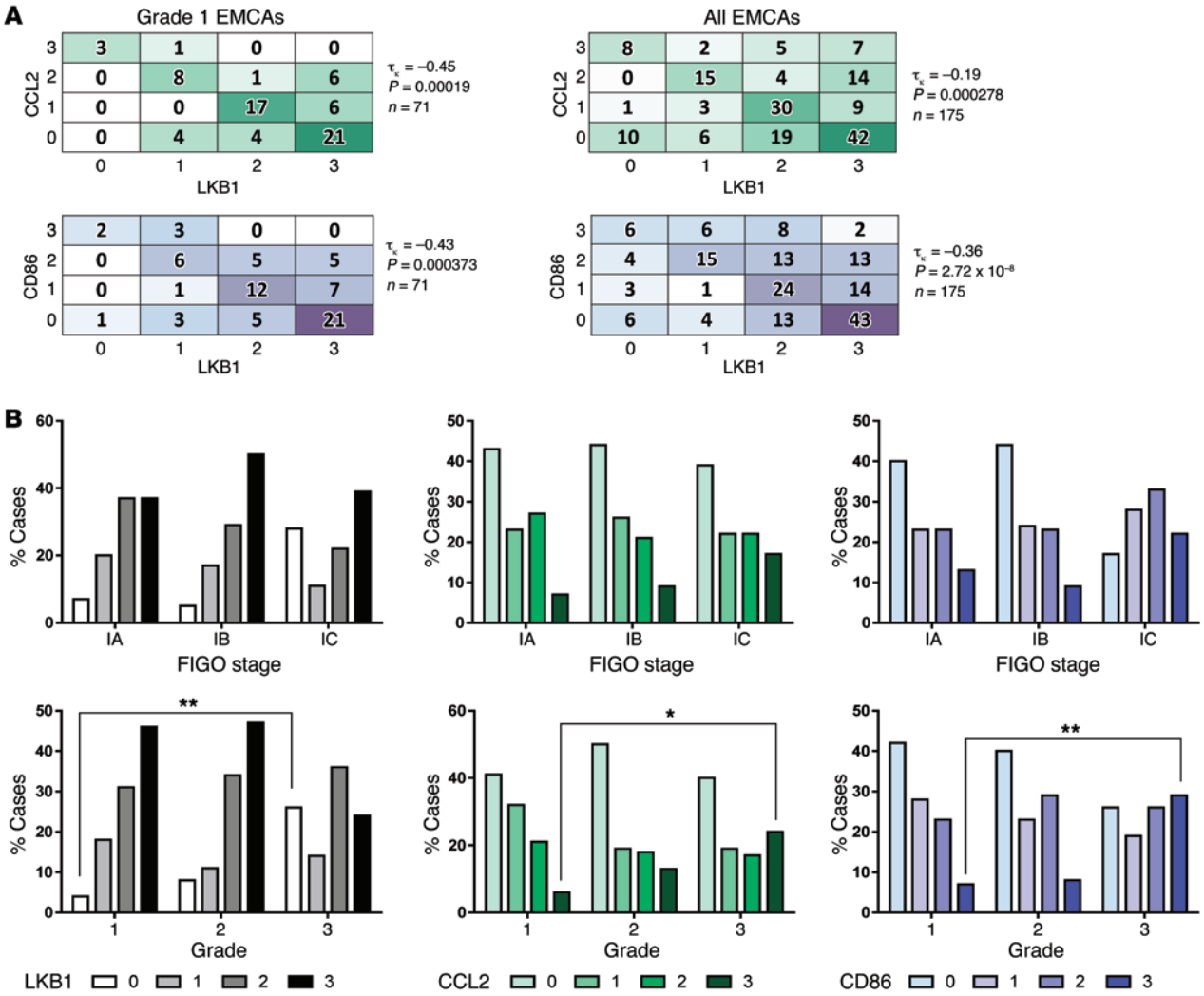

Figure 8. Low LKB1 protein levels in primary human endometrial cancers are strongly correlated with high CCL2 expression and increased macrophage density. A human endometrial cancer TMA was stained and scored for each marker per the schematic in Supplemental Figure 6. A total of 175 separate cases of primary endometrial cancer were scored. Pair-wise correlations were evaluated by Kendall's τ coefficient, with P values determined by 2-tailed t tests. (**A**) Heat maps showing significant negative correlations among grade 1 and grade 1–3 endometrial adenocarcinomas. (**B**) Top panels: number of cases with specific staining scores (grades 0–3) among tumors of different clinical stages (FIGO 1A, 1B, 1C). Of cases with more than 50% myometrial invasion (defined as stage 1C), the percentage with low LKB1 expression or high CCL2/CD68 expression was significantly increased. Bottom panels: number of cases with specific staining scores (grades 0–3) among tumors of different histopathological grades (grades 1, 2, 3). There was a significantly greater percentage of cases expressing low levels of LKB1 protein among high-grade tumors (n = 113). Additionally, there was a significantly greater percentage of cases expressing high levels of CCL2 (n = 113) and CD68 (n = 113) among high-grade tumors. *P < 0.005; **P < 0.001, Fisher's exact t test.

through less than half of the myometrium and 1C tumors invade through greater than half of the myometrial thickness (66). There was a trend toward higher numbers of cases with low LKB1 (protein score = 0) expression among stage 1C cases, although this did not achieve statistical significance. However, there was a statistically significant (P < 0.001) increase in cases with low LKB1 expression in grade 3 versus grade 1. For CCL2 and CD68, there was again a trend toward increased expression in stage 1C versus 1A that did not achieve significance, while there was a statistically significant increase in cases expressing high levels of these cancers in grade 1 versus grade 3 tumors (P < 0.005, Figure 8B). These studies, conducted in a large set of human primary endometrial cancers, provide strong support for a model where LKB1 loss promotes tumor progression through increased CCL2 secretion by the primary tumor, leading to increased macrophage recruitment to the tumor. Prior studies also consistently demonstrated a strong association between TAM density in primary endometrial tumors and grade, stage, and clinical outcome (67–70).

Discussion

At the initiation of these studies, the paradoxically aggressive phenotypes we had previously described for LKB1-deficient uterine cancers (8, 11) strongly suggested that LKB1 acted as a uterine tumor suppressor via unknown biological mechanisms. This study, which began with expression profiling of isogenic cell lines to pinpoint such biological pathways, demonstrated that LKB1 regulates the transcription of multiple secreted factors of potential relevance to LKB1's actions as a tumor suppressor. Additional

investigations, which included analyses of a genetically engineered mouse model as well as primary human tumors, led to the unexpected discovery that one of these factors — the chemokine CCL2 — is a physiologically important effector of Lkb1-driven endometrial cancers. Our studies revealed an unanticipated but essential role for LKB1 in the control of the TME in addition to the well-known effects of LKB1 on cell-autonomous metabolism and signaling. Specifically, we showed that LKB1 loss in EM cells leads to increased expression and secretion of CCL2 in a cell-autonomous manner and that increased intratumoral CCL2 derived from epithelial cells in turn leads to accelerated tumor growth via the recruitment of protumorigenic macrophages. Our study thus forges new links among endometrial carcinogenesis, the LKB1 tumor suppressor, CCL2/CCR2, and TAMs and provides insights into the particularly aggressive tumor phenotypes associated with LKB1 loss.

Our data are in line with growing evidence implicating inflammatory chemokines in general, and CCL2 in particular, with tumor progression. Chronic inflammation is a hallmark of cancer and linked with the initiation and progression of carcinomas. In carcinomas of the breast, prostate, colon, liver, and bladder, production of CCL2 by tumor cells is associated with increased infiltration of TAMs and early clinical relapse (38, 71). For example, in uterine cervical cancer, absence of *CCL2* mRNA expression correlated with decreased TAM density and improved overall survival (72). Our study is thus consistent with prior data showing that CCL2 expression is a significant prognostic factor in cancer (38).

A variety of cell-surface receptors expressed on monocytes/macrophages together with their corresponding ligands, including CCR2/CCL2, VEGFR1/VEGF-A, and CX3CR1/CX3CL1, regulate monocyte recruitment into tumors. In general, the expression of one or more of these ligands positively correlates with TAM numbers. CCL2 is a potent chemoattractant of monocytes/macrophages and appears to be the main determinant of monocyte/macrophage recruitment within primary tumors. CCL2 production in distant metastatic deposits can also lead to the recruitment of monocytes and thereby promote growth of these deposits (73). Normal, uninjured tissues produce low levels of CCL2, whereas tumors often express and produce higher CCL2 levels. Some monocyte chemoattractants (e.g., VEGF-A) are produced within carcinomas by nonepithelial cells (such as fibroblasts). In contrast, CCL2 is largely produced by the malignant epithelial cells, although other cells in the primary TME can also serve as sources of CCL2.

In our model, CCL2 produced by the primary endometrial cancer was detectable in the circulation. Furthermore, increased circulating monocytes were observed in these *Lkb1*$^{-/-}$ female mice, consistent with the well-established role of the CCL2/CCR2 axis in the mobilization of monocytes from the bone marrow to the blood (74) and further signifying that the CCL2 produced by tumors can exert systemic as well as local effects. Consistent with this idea, serum CCL2 (sCCL2) represents a potential circulating biomarker to monitor tumor progression or predict progression risk. In patients with gastric and hepatocellular carcinomas, preoperative levels of sCCL2 were significantly higher than in control patients and correlated with stage (75). However, studies of sCCL2 in cancer are in their early stages, and data on sCCL2 circulating levels in women with endometrial cancer are not yet available.

CCL2 produced by malignant epithelial cells within a tumor serves to recruit monocytes and promote their differentiation (paracrine effects), but can also directly affect the malignant cells themselves (autocrine effects). High-grade urothelial (bladder) carcinomas expressing high levels of CCL2 stimulate their own growth, migration, and invasive capacity in a cell-autonomous, CCR2-dependent manner (38). CCL2 also promotes prostate cancer chemotaxis, invasion, and metastasis via CCR2 and its downstream effectors, which include PI3K/AKT, Rac, and RhoA (71). Although we did not directly evaluate the contributions of such CCL2-dependent autocrine mechanisms on endometrial cancer progression in our models, we have documented expression of the CCR2 receptor protein in all uterine cancer cell lines we have analyzed, including both endometrial and cervical cancer cell lines (our unpublished observations). Thus, we believe that such autocrine effects are not only plausible but likely and deserve further investigation. Another intriguing possibility is that CCL2/CCR2 interactions could have cell-autonomous effects on intracellular metabolism, which might in turn further synergize with the LKB1/AMPK/mTOR axis. The specific mechanisms and signaling cascades by which the LKB1/AMPK axis regulates CCL2 expression also remain an important area of inquiry deserving further investigations.

Increased TAM density in human endometrial cancer is associated with a worse clinical prognosis. Macrophages are the most abundant leukocyte population in mouse and human endometrium, where they serve diverse physiologic functions during endometrial cycling and pregnancy. In a large recent study of $n = 163$ primary endometrial cancers, increased TAM density correlated strongly with advanced tumor stage and grade, lymphovascular space involvement, and decreased recurrence-free and overall survival. Interestingly, intratumoral density of other immune cellular subsets, such as Tregs, did not correlate with these clinical parameters (70). Both our mouse and human studies confirm that TAMs in primary endometrial tumors have protumorigenic roles and implicate the LKB1/AMPK axis as an important regulator of TAM density in tumors via CCL2.

CCL2 exerts its biological roles principally via CCR2, which is highly expressed in classical monocytes. Conversely, CCR2 is not known to be activated by any chemokines other than CCL2. This mutual relationship suggests that, for tumors characterized by high levels of CCL2, inhibition of CCR2 through neutralizing antibodies or through small molecule drugs in clinical development might prove a useful therapeutic approach (76). New therapeutic strategies for endometrial cancer are urgently needed, as there are as yet no curative treatments for advanced disease, although recently, objective responses have been documented for temsirolimus, an mTOR inhibitor (77). Our study and prior data demonstrating that TAM density is an important driver of human endometrial tumor progression lend further support to the notion that the LKB1/CCL2/TAM axis is an attractive target for new therapeutic strategies. Our demonstration that genetic inactivation of *Ccl2* suppresses *Lkb1*-driven tumors in vivo also lends strong support for this idea. Further validation for anti-CCL2/CCR2 therapeutic strategies and additional biological insights are likely to be gained by additional investigations of the *Lkb1*$^{-/-}$ mouse model, particularly since the complete penetrance of endometrial adenocarcinomas and stereotypical tumor progression make this a high-

ly tractable model. Taken together, our data indicate that *Lkb1*$^{-/-}$ mice should serve as an optimal preclinical platform for testing diverse agents currently in various stages of clinical development, including CCL2- or CCR2-neutralizing antibodies or small molecule inhibitors that target CCR2. It will also be interesting to test the efficacy of such agents either alone or in combination with agents (such as temsirolimus) likely to synergize with LKB1 loss and the ensuing hyperactivation of AMPK/mTOR pathways (11).

Methods

Creation of stable, LKB1 knockdown cell lines by lentiviral shRNA. Nonoverlapping LKB1 shRNA sequences (shRNA1, 5′-CCGGGCCAACGTGAAGAAGGAAATTCTCGAGAATTTCCTTCTTCACGTTGGCTTTTT-3′; shRNA2, 5′-CCGGGATCCTCAAGAAGAAGAAGTTCTCGAGAACTTCTTCTTCTTGAGGATCTTTTT-3′; underlines indicate complementary 21-bp stem sequences corresponding to *LKB1* genomic sequences) were cloned into AgeI-EcoRI sites of the pLKO.1 vector (Sigma-Aldrich, catalog SHC002). FuGENE HD transfection reagent (Promega, catalog E2311) was used to cotransfect each shRNA vector or a nontarget control vector (Sigma-Aldrich, catalog SCH001) with lentiviral packaging plasmid (psPAX2, Addgene catalog 12260) and VSV-G envelope–expressing plasmid (pMD2.G, Addgene catalog 12259) into HEC293T cells for 15 hours. Transfection medium was replaced and incubated in fresh media at 37°C for 24 hours to produce lentivirus particles.

An immortalized, endometrial epithelial cell line (EM cells) obtained from Masaki Inoue (Kanazawa School of Medicine, Tokyo, Japan) (34) was grown in DMEM/F-12, HEPES buffer (Life Technologies, catalog 11330) supplemented with 10% FBS. 150,000 EM cells were individually infected with lentivirus (nontarget, shRNA1, or shRNA2) for 24 hours with polybrene (4 μg/ml) (Sigma-Aldrich, catalog H9268), followed by replacement with fresh medium. Stably transfected cells were selected with 1 μg/ml puromycin (Clontech, catalog 631305) over 1.5 weeks. Three biological replicates of EM cells per lentivirus were created to produce a total of 9 cell lines.

For AMPK knockdown experiments, this process was repeated using either control shRNA lentiviral particles (Santa Cruz Biotechnology Inc., catalog sc1080-80) or AMPKα1/2 shRNA lentiviral particles (Santa Cruz Biotechnology Inc., catalog sc-45312-V).

RNA preparation and qRT-PCR. Total mRNA was isolated from EM cells using the RNeasy Mini Kit (QIAGEN, catalog 74104). cDNA (0.5 μg) was synthesized using mRNA via Superscript VILO (Life Technologies, catalog 11754) and diluted in TaqMan Universal PCR Master Mix (Life Technologies, catalog 4304437) with TaqMan probes (Life Technologies, catalog 4453320) including MXRA5 (Hs01019147_m1), LKB1 (Hs00176092_m1), CRIP2 (Hs00373842_g1), GCNT2 (Hs00377334_m1), FABP4 (Hs01086177_m1), CXCL6 (Hs00605742_g1), FST (Hs00246256_m1), and CCL2 (Hs00234140_m1). qRT-PCR was performed on master mixes in triplicate using Applied Biosystems StepOnePlus Real-Time PCR machine. Ct values per gene were averaged before computing fold change by the ΔΔCt method using GAPDH as a reference gene and EM nontarget shRNA cells as reference samples.

Microarray and gene ontology analysis. Microarray hybridization was performed per the manufacturer's specifications with 500 ng of labeled total RNA. Preparation of samples and loading of RNA onto the HumanHT-12 v4 Expression BeadChip was performed by the UTSW DNA Microarray Core Facility. Three biological replicates of RNA from nontarget, shRNA1, and shRNA2 cells were loaded onto the chip. All original microarray data were deposited in the NCBI's Gene Expression Omnibus (GEO GSE67629).

Array analysis was performed using Illumina GenomeStudio 2011 software v2011.1. A 95% confidence interval was used to filter out nonspecific binding of probes to RNA. Probe intensities of shRNA1 or shRNA2 were normalized to nontarget probe intensities, and resultant values of less than 3× were excluded. Intensity values that differed in directionality between shRNA1 and shRNA2 were additionally filtered out, leaving 59 probe sets unique to shRNA1, 142 probe sets unique to shRNA2, and 43 probe sets in common. Gene ontology analysis was performed on tabulated genes from the filtered probe sets using WebGestalt (78).

Lysate preparation for immunoblotting and ELISA. Cells in culture were washed in PBS following media aspiration. Cells were mechanically detached from culture dishes in RIPA buffer (Pierce, catalog 89900) supplemented with protease (Roche, catalog 11836170001) and phosphatase inhibitors (Sigma-Aldrich, catalog P5726) on ice. Normal and cancerous uteri were rinsed in PBS before homogenization in RIPA buffer. Protein from cells and tissue lysate was quantified using the Pierce BCA Protein Assay Kit (catalog 23227). Equal amounts of protein were used for Western blots and ELISA. ELISA for murine tumor lysate and sCCL2 was performed using the Mouse/Rat CCL2/JE/MCP-1 Quantikine ELISA Kit per the manufacturer's instructions (R&D Systems, catalog MJE00).

In vitro cell culture studies. EM cells (nontarget, shRNA1, shRNA2) were plated at 75,000 cells/plate in 6-well plates (Corning, catalog CLS3516). Cells were allowed to grow for 24 hours, rinsed in PBS, and replaced with fresh medium containing either PBS (vehicle), 0.5 mM AICAR (Sigma-Aldrich, catalog A9978), or 5 mM metformin (Sigma-Aldrich, catalog PHR1084). Lysates and conditioned media were harvested from cells 24 hours after drug treatment. Western blotting on lysates (including nondrug studies) was done using 1:1000 dilutions of the following antibodies (Cell Signaling Technologies) in Tris-buffered saline containing 5% milk: LKB1 (catalog D60C5), pAMPK (Thr172) (catalog 2535), AMPK (catalog 2603), pS6 (catalog 4857), S6 (catalog 2217), p4EBP1 (catalog 9455), 4EBP1 (catalog 9452), and GAPDH (catalog 2118). ELISA on conditioned media (including nondrug studies) for CCL2 was performed using the Human CCL2/MCP-1 Quantikine ELISA Kit according to the manufacturer's instructions (R&D Systems, catalog DCP00).

Growth and migration assays were as described (3). CCL2 cDNA subcloned into a pDream2.1 plasmid was obtained (Genescript, catalog SD0222). Transfection into Ishikawa cells (Sigma-Aldrich, catalog 99040201-1VL) was performed with Lipofectamine reagent (Life Technologies, catalog 11668) per the manufacturer's instructions. Agarose plugs for testing of IHC protocols were prepared as described (65).

Mouse husbandry and procedures involving tissues or live animals. Mice were housed in a pathogen-free animal facility in microisolator cages and fed ad libitum on standard chow. Control animals (*Lkb1*$^{f/f}$) and *Lkb1*$^{-/-}$ endometrial *Lkb1*-knockout mice (FVB/n genetic background, backcrossed > 10 generations) were bred and generated as previously described (11). *Ccl2*$^{-/-}$ mice (B6.129S4-Ccl2^{tm1Rol}/J) were obtained from Jackson Laboratories. Tissue sections from *Pten* and *Pten/Mig-6* uteri were a gift from Jae-Wook Jeong (Michigan State University, East Lansing, Michigan, USA) (49–54). Mouse blood was obtained by retroorbital bleeding and collected in EDTA tubes for

CBCs (IDEXX ProCyte Dx Hematology Analyzer) or in Eppendorf tubes and allowed to coagulate before serum collection. ELISA for murine tumor lysate and sCCL2 was performed using the Mouse/Rat CCL2/JE/MCP-1 Quantikine ELISA Kit per the manufacturer's instructions (R&D Systems, catalog MJE00).

Nine-week-old *Lkb1*$^{-/-}$ females were treated with intraperitoneal injections of liposomal clodronate or liposomal PBS (0.4 ml of suspension per 25 g animal weight 4 times a week) for 9 weeks. Liposomal clodronate and control liposomes were purchased from Clodronate Liposomes.

Tissue processing, IHC, immunofluorescence. Fixation, sectioning, antigen retrieval, blocking, and secondary detection for the following antibody dilutions in 2% BSA were performed as previously described (65): LKB1 (1:10,000 human tissue, 1:5000 mouse tissue, Cell Signaling Technologies, catalog D60C5F10), CD68 (1:250, Dako, catalog M0876), CCL2 (1:250, Sigma-Aldrich, catalog HPA019163), MYP (1:250, Abcam, catalog ab9535), CD3 (1:50, Abcam, catalog ab5690) and pAMPK (Thr172) (1:75, Cell Signaling Technologies, catalog 2535). Antigen retrieval for F4/80 immunostaining (1:100, Abd Serotec, catalog MCA497) on PEFFT was performed using 0.005% pepsin in 0.01 M HCl at 37°C for 15 minutes, followed by water and PBS rinses. Blocking and secondary detection for F4/80 were performed as described (65).

Immunofluorescence was performed by embedding frozen tissues in OCT and cryosectioning, followed by 5-minute fixation in cold acetone, and blocking in 3% BSA prior to the following antibody dilutions in 3% BSA: rat anti-mouse F4/80 (1:100, Abd Serotec), goat anti-mouse CD163 (1:50, Santa Cruz Biotechnology Inc., catalog sc33560), rabbit anti-mouse Arg1 (1:100, Santa Cruz Biotechnology Inc., catalog sc18351), and rat anti-mouse CCL2 (1:50, Clone ECE2, Novus Biologicals, catalog NBP1-42312). Secondary antibodies (Life Technologies) included the following: Alexa Fluor 488 donkey anti-rat (catalog A21208), Alexa Fluor 488 donkey anti-goat (catalog A11055), and Alexa Fluor 555 goat anti-rabbit (catalog A21429).

Flow cytometry. Cell suspensions were obtained from mice by enzymatic digestion and washed in FACS buffer (1% BSA, 0.01% NaN_3 in PBS). Cells were blocked for 5 minutes with Fc blocking reagent (BD Biosciences — Pharmingen, catalog 553142) prior to labeling with fluorescent-conjugated antibodies diluted in FACS buffer: F4/80-PerCy5.5 (1:200, Tonbo Biosciences, catalog 65-4801) and CCR2-APC (1:50, R&D Systems, catalog FAB5538A). Flow cytometry was performed using a FACSCalibur and the results were analyzed with FlowJo software.

Histological scoring scheme for TMA. The generation of TMA was previously described (10). A 4-category classification scheme was employed to score protein expression for LKB1 and CCL2 based on the staining intensity within epithelium. For CD68, scoring reflected macrophage numbers in stroma and epithelium. The 4 categories for CD68 were as follows: 0 ≤ 100 macrophages; 1 = 101–200; 2 = 201–300; and 3 > 300 total macrophages per intact core.

Statistics. Data are presented as mean ± SEM unless otherwise indicated. To determine *P* values, 2-tailed Student's *t* tests were performed (unless otherwise indicated). $P < 0.05$ was considered statistically significant. For survival curves, Kaplan-Meier analysis was used, with statistical comparison among curves performed with the log-rank test. Overlap among the 2 shRNA gene sets was calculated by the hypergeometric test. Kendall's τ correlation coefficients were calculated using Wessa statistics software. Routine statistical analyses were performed with either GraphPad Prism (version 6.05) or Microsoft Excel. No statistical method was used to predetermine sample size. The experiments were not randomized, and the investigators were not blinded to allocation during experiments and outcome assessment.

Study approval. Animal studies were approved by the University of Texas Southwestern IACUC. Use of human samples was exempt from IRB approval due to the use only of anonymized, archival specimens. Experiments were conducted with the approval of and under the guidelines of the University of Texas Southwestern Environmental Health and Safety Office.

Acknowledgments

We thank the David M. Crowley Foundation for support and members of the Castrillon laboratory for critically reading the manuscript. We also thank Jae-Wook Jeong for providing tissue samples. This work was supported by grants to D.H. Castrillon from the NIH (R01CA137181) and the Cancer Prevention & Research Institute of Texas (RP100550) and by a grant from the NIH (U01CA141576) to D.H. Castrillon and K.K. Wong.

Address correspondence to: Diego H. Castrillon, 5323 Harry Hines Blvd., Dallas, Texas 75390-9072, USA. Phone: 214.648.4032; E-mail: diego.castrillon@utsouthwestern.edu.

1. Hemminki A, et al. A serine/threonine kinase gene defective in Peutz-Jeghers syndrome. *Nature*. 1998;391(6663):184–187.
2. Hearle N, et al. Frequency and spectrum of cancers in the Peutz-Jeghers syndrome. *Clin Cancer Res*. 2006;12(10):3209–3215.
3. Liu W, et al. LKB1/STK11 inactivation leads to expansion of a prometastatic tumor subpopulation in melanoma. *Cancer Cell*. 2012;21(6):751–764.
4. Guldberg P, thor Straten P, Ahrenkiel V, Seremet T, Kirkin AF, Zeuthen J. Somatic mutation of the Peutz-Jeghers syndrome gene, LKB1/STK11, in malignant melanoma. *Oncogene*. 1999;18(9):1777–1780.
5. Alessi DR, Sakamoto K, Bayascas JR. Lkb1-dependent signaling pathways. *Annu Rev Biochem*. 2006;75:137–163.
6. Ji H, et al. LKB1 modulates lung cancer differentiation and metastasis. *Nature*. 2007;448(7155):807–810.
7. Ding L, et al. Somatic mutations affect key pathways in lung adenocarcinoma. *Nature*. 2008;455(7216):1069–1075.
8. Wingo SN, et al. Somatic LKB1 mutations promote cervical cancer progression. *PLoS One*. 2009;4(4):e5137.
9. Zhao N, et al. Alterations of LKB1 and KRAS and risk of brain metastasis: comprehensive characterization by mutation analysis, copy number, and gene expression in non-small-cell lung carcinoma. *Lung Cancer*. 2014;86(2):255–261.
10. Contreras CM, et al. Loss of Lkb1 provokes highly invasive endometrial adenocarcinomas. *Cancer Res*. 2008;68(3):759–766.
11. Contreras CM, et al. Lkb1 inactivation is sufficient to drive endometrial cancers that are aggressive yet highly responsive to mTOR inhibitor monotherapy. *Dis Model Mech*. 2010;3(3–4):181–193.
12. Ollila S, Makela TP. The tumor suppressor kinase LKB1: lessons from mouse models. *J Mol Cell Biol*. 2011;3(6):330–340.
13. Gaude H, et al. Molecular chaperone complexes with antagonizing activities regulate stability and activity of the tumor suppressor LKB1. *Oncogene*. 2012;31(12):1582–1591.
14. Boudeau J, Deak M, Lawlor MA, Morrice NA, Alessi DR. Heat-shock protein 90 and Cdc37 interact with LKB1 and regulate its stability. *Biochem J*. 2003;370(pt 3):849–857.
15. Bouchekioua-Bouzaghou K, et al. LKB1 when associated with methylatedERa is a marker of bad prognosis in breast cancer. *Int J Cancer*. 2014;135(6):1307–1318.
16. Tsai LH, et al. LKB1 loss by alteration of the NKX2-

1/p53 pathway promotes tumor malignancy and predicts poor survival and relapse in lung adenocarcinomas. *Oncogene*. 2014;33(29):3851–3860.
17. Huang YH, et al. Decreased expression of LKB1 correlates with poor prognosis in hepatocellular carcinoma patients undergoing hepatectomy. *Asian Pac J Cancer Prev*. 2013;14(3):1985–1988.
18. He TY, Tsai LH, Huang CC, Chou MC, Lee H. LKB1 loss at transcriptional level promotes tumor malignancy and poor patient outcomes in colorectal cancer. *Ann Surg Oncol*. 2014;21(suppl 4):S703–S710.
19. Cancer Genome Atlas Research Network, et al. Integrated genomic characterization of endometrial carcinoma. *Nature*. 2013;497(7447):67–73.
20. Gill RK, et al. Frequent homozygous deletion of the LKB1/STK11 gene in non-small cell lung cancer. *Oncogene*. 2011;30(35):3784–3791.
21. Morton JP, et al. LKB1 haploinsufficiency cooperates with Kras to promote pancreatic cancer through suppression of p21-dependent growth arrest. *Gastroenterology*. 2010;139(2):586–597.
22. Shackelford DB, Shaw RJ. The LKB1-AMPK pathway: metabolism and growth control in tumour suppression. *Nat Rev Cancer*. 2009;9(8):563–575.
23. Hardie DG, Ross FA, Hawley SA. AMPK: a nutrient and energy sensor that maintains energy homeostasis. *Nat Rev Mol Cell Biol*. 2012;13(4):251–262.
24. Courchet J, et al. Terminal axon branching is regulated by the LKB1-NUAK1 kinase pathway via presynaptic mitochondrial capture. *Cell*. 2013;153(7):1510–1525.
25. Chan KT, et al. LKB1 loss in melanoma disrupts directional migration toward extracellular matrix cues. *J Cell Biol*. 2014;207(2):299–315.
26. Faubert B, et al. AMPK is a negative regulator of the Warburg effect and suppresses tumor growth in vivo. *Cell Metab*. 2013;17(1):113–124.
27. Xu C, et al. Loss of Lkb1 and Pten leads to lung squamous cell carcinoma with elevated PD-L1 expression. *Cancer Cell*. 2014;25(5):590–604.
28. Komiya T, et al. Enhanced activity of the CREB co-activator Crtc1 in LKB1 null lung cancer. *Oncogene*. 2010;29(11):1672–1680.
29. Cao C, et al. Role of LKB1-CRTC1 on glycosylated COX-2 and response to COX-2 inhibition in lung cancer. *J Natl Cancer Inst*. 2015;107(1):358.
30. Greer EL, et al. The energy sensor AMP-activated protein kinase directly regulates the mammalian FOXO3 transcription factor. *J Biol Chem*. 2007;282(41):30107–30119.
31. Goodwin JM, Svensson RU, Lou HJ, Winslow MM, Turk BE, Shaw RJ. An AMPK-independent signaling pathway downstream of the LKB1 tumor suppressor controls Snail1 and metastatic potential. *Mol Cell*. 2014;55(3):436–450.
32. Tsai LH, et al. The MZF1/c-MYC axis mediates lung adenocarcinoma progression caused by wild-type lkb1 loss. *Oncogene*. 2015;34(13):1641–1649.
33. Jacob LS, et al. Genome-wide RNAi screen reveals disease-associated genes that are common to Hedgehog and Wnt signaling. *Sci Signal*. 2011;4(157):ra4.
34. Kyo S, et al. Successful immortalization of endometrial glandular cells with normal structural and functional characteristics. *Am J Pathol*. 2003;163(6):2259–2269.
35. Carretero J, et al. Integrative genomic and proteomic analyses identify targets for Lkb1-deficient metastatic lung tumors. *Cancer Cell*. 2010;17(6):547–559.
36. Zhuang ZG, Di GH, Shen ZZ, Ding J, Shao ZM. Enhanced expression of LKB1 in breast cancer cells attenuates angiogenesis, invasion, and metastatic potential. *Mol Cancer Res*. 2006;4(11):843–849.
37. Ossipova O, Bardeesy N, DePinho RA, Green JB. LKB1 (XEEK1) regulates Wnt signalling in vertebrate development. *Nat Cell Biol*. 2003;5(10):889–894.
38. Borsig L, Wolf MJ, Roblek M, Lorentzen A, Heikenwalder M. Inflammatory chemokines and metastasis — tracing the accessory. *Oncogene*. 2014;33(25):3217–3224.
39. Tsuyada A, et al. CCL2 mediates cross-talk between cancer cells and stromal fibroblasts that regulates breast cancer stem cells. *Cancer Res*. 2012;72(11):2768–2779.
40. Zhang J, Patel L, Pienta KJ. Targeting chemokine (C-C motif) ligand 2 (CCL2) as an example of translation of cancer molecular biology to the clinic. *Prog Mol Biol Transl Sci*. 2010;95:31–53.
41. Zhou G, et al. Role of AMP-activated protein kinase in mechanism of metformin action. *J Clin Invest*. 2001;108(8):1167–1174.
42. Sullivan JE, Brocklehurst KJ, Marley AE, Carey F, Carling D, Beri RK. Inhibition of lipolysis and lipogenesis in isolated rat adipocytes with AICAR, a cell-permeable activator of AMP-activated protein kinase. *FEBS Lett*. 1994;353(1):33–36.
43. Hawley SA, et al. Calmodulin-dependent protein kinase kinase-β is an alternative upstream kinase for AMP-activated protein kinase. *Cell Metab*. 2005;2(1):9–19.
44. Bardeesy N, et al. Loss of the Lkb1 tumour suppressor provokes intestinal polyposis but resistance to transformation. *Nature*. 2002;419(6903):162–167.
45. Zhu X, et al. Myeloid cell-specific ABCA1 deletion protects mice from bacterial infection. *Circ Res*. 2012;111(11):1398–1409.
46. Lizcano JM, et al. LKB1 is a master kinase that activates 13 kinases of the AMPK subfamily, including MARK/PAR-1. *EMBO J*. 2004;23(4):833–843.
47. Shaw RJ, et al. The LKB1 tumor suppressor negatively regulates mTOR signaling. *Cancer Cell*. 2004;6(1):91–99.
48. Pollard JW, Lin EY, Zhu L. Complexity in uterine macrophage responses to cytokines in mice. *Biol Reprod*. 1998;58(6):1469–1475.
49. Jeong JW, et al. β-Catenin mediates glandular formation and dysregulation of beta-catenin induces hyperplasia formation in the murine uterus. *Oncogene*. 2009;28(1):31–40.
50. Kim TH, et al. The synergistic effect of Mig-6 and Pten ablation on endometrial cancer development and progression. *Oncogene*. 2010;29(26):3770–3780.
51. Kim TH, et al. Critical tumor suppressor function mediated by epithelial Mig-6 in endometrial cancer. *Cancer Res*. 2013;73(16):5090–5099.
52. Kim TH, et al. Mig-6 suppresses endometrial cancer associated with Pten deficiency and ERK activation. *Cancer Res*. 2014;74(24):7371–7382.
53. Lee TH, et al. Peroxiredoxin II is essential for sustaining life span of erythrocytes in mice. *Blood*. 2003;101(12):5033–5038.
54. Yoo JY, Kim TH, Lee JH, Dunwoodie SL, Ku BJ, Jeong JW. Mig-6 regulates endometrial genes involved in cell cycle and progesterone signaling. *Biochem Biophys Res Commun*. 2015;462(4):409–414.
55. Akbay EA, et al. Differential roles of telomere attrition in type I and II endometrial carcinogenesis. *Am J Pathol*. 2008;173(2):536–544.
56. Akbay EA, et al. Cooperation between p53 and the telomere-protecting shelterin component Pot1a in endometrial carcinogenesis. *Oncogene*. 2013;32(17):2211–2219.
57. Comito G, et al. Cancer-associated fibroblasts and M2-polarized macrophages synergize during prostate carcinoma progression. *Oncogene*. 2014;33(19):2423–2431.
58. Mantovani A, Sozzani S, Locati M, Allavena P, Sica A. Macrophage polarization: tumor-associated macrophages as a paradigm for polarized M2 mononuclear phagocytes. *Trends Immunol*. 2002;23(11):549–555.
59. Colegio OR, et al. Functional polarization of tumour-associated macrophages by tumour-derived lactic acid. *Nature*. 2014;513(7519):559–563.
60. Pesce JT, et al. Arginase-1-expressing macrophages suppress Th2 cytokine-driven inflammation and fibrosis. *PLoS Pathog*. 2009;5(4):e1000371.
61. van Rooijen N, Hendrikx E. Liposomes for specific depletion of macrophages from organs and tissues. *Methods Mol Biol*. 2010;605:189–203.
62. Danenberg HD, et al. Macrophage depletion by clodronate-containing liposomes reduces neointimal formation after balloon injury in rats and rabbits. *Circulation*. 2002;106(5):599–605.
63. Lu B, et al. Abnormalities in monocyte recruitment and cytokine expression in monocyte chemoattractant protein 1-deficient mice. *J Exp Med*. 1998;187(4):601–608.
64. Deshmane SL, Kremlev S, Amini S, Sawaya BE. Monocyte chemoattractant protein-1 (MCP-1): an overview. *J Interferon Cytokine Res*. 2009;29(6):313–326.
65. Nakada Y, et al. The LKB1 tumor suppressor as a biomarker in mouse and human tissues. *PLoS One*. 2013;8(9):e73449.
66. Mikuta JJ. International Federation of Gynecology and Obstetrics staging of endometrial cancer 1988. *Cancer*. 1993;71(4 suppl):1460–1463.
67. Espinosa I, et al. Myometrial invasion and lymph node metastasis in endometrioid carcinomas: tumor-associated macrophages, microvessel density, and HIF1A have a crucial role. *Am J Surg Pathol*. 2010;34(11):1708–1714.
68. Ohno S, et al. Correlation of histological localization of tumor-associated macrophages with clinicopathological features in endometrial cancer. *Anticancer Res*. 2004;24(5C):3335–3342.
69. Soeda S, et al. Tumor-associated macrophages correlate with vascular space invasion and myometrial invasion in endometrial carcinoma. *Gynecol Oncol*. 2008;109(1):122–128.
70. Kubler K, et al. Prognostic significance of tumor-associated macrophages in endometrial adenocarcinoma. *Gynecol Oncol*. 2014;135(2):176–183.

71. Zhang J, Lu Y, Pienta KJ. Multiple roles of chemokine (C-C motif) ligand 2 in promoting prostate cancer growth. *J Natl Cancer Inst*. 2010;102(8):522–528.
72. Zijlmans HJ, Fleuren GJ, Baelde HJ, Eilers PH, Kenter GG, Gorter A. The absence of CCL2 expression in cervical carcinoma is associated with increased survival and loss of heterozygosity at 17q11. *J Pathol*. 2006;208(4):507–517.
73. Qian BZ, et al. CCL2 recruits inflammatory monocytes to facilitate breast-tumour metastasis. *Nature*. 2011;475(7355):222–225.
74. Shi C, Pamer EG. Monocyte recruitment during infection and inflammation. *Nat Rev Immunol*. 2011;11(11):762–774.
75. Wang WW, et al. Identification of serum monocyte chemoattractant protein-1 and prolactin as potential tumor markers in hepatocellular carcinoma. *PLoS One*. 2013;8(7):e68904.
76. Struthers M, Pasternak A. CCR2 antagonists. *Curr Top Med Chem*. 2010;10(13):1278–1298.
77. Alvarez EA, et al. Phase II trial of combination bevacizumab and temsirolimus in the treatment of recurrent or persistent endometrial carcinoma: a Gynecologic Oncology Group study. *Gynecol Oncol*. 2013;129(1):22–27.
78. Zhang B, Kirov S, Snoddy J. WebGestalt: an integrated system for exploring gene sets in various biological contexts. *Nucleic Acids Res*. 2005;33(Web Server issue):W741–W748.